Vol 16 No 7, July 2007
1009-1963/2007/16(07)/2003-08
Chinese Physics
© 2007 Chin. Phys. Soc.
and IOP Publishing Ltd

A study of ultrafast electron diffusion kinetics in ultrashort-pulse laser ablation of metals*

Yang Jian-Jun(杨建军)[a)†], Liu Wei-Wei(刘伟伟)[a)b)], and Zhu Xiao-Nong(朱晓农)[a)]

[a)] *Institute of Modern Optics, Nankai University, Key Laboratory of Opto-Electronic Information Science and Technology, Education Ministry of China, Tianjin* 300071, *China*

[b)] *Department de Physique, de Genie Physique et D'Optique and Centre d'Optique, Photonique et Laser, Universite Laval, Quebec G1K 7P4, Canada*

(Received 30 November 2006; revised manuscript received 11 January 2007)

Temperature dependence of the electron diffusion in metallic targets, where the electron–electron collision is the dominant process, is investigated with the help of an extended two-temperature model. In sharp contrast to the low electron temperature case, where only the electron—phonon collisions are commonly considered, the electron diffusion process underlying the high electron temperatures evolves dramatically different in both temporal and spatial domains. Calculated results of the ablation yield at different pulse durations are presented for a copper plate impinged by ultrashort laser pulses with energy fluences ranging from 0.1 J/cm^2 to 10 J/cm^2. The excellent agreement between the simulation results and the experimental data indicates the significant role of electron–electron collisions in material ablations using intense ultrashort laser pulses.

Keywords: electron diffusion, femtosecond pulse, ablation
PACC: 4262A, 7890, 8140T

1. Introduction

Femtosecond pulse lasers have opened up many new opportunities for the study of ultrafast phenomena such as hot electron dynamics and electron–phonon coupling in condensed matters.[1−3] Although some important thermal dynamic behaviours already have been clarified in experiments by using low-energy laser pulses, the fast electron relaxation dynamics associated with high-intensity femtosecond laser excitation remains to be explored.[4] For example, in the experiment of femtosecond heating of thin gold films reported by Brorson,[5] a nondiffusion-like ballistic heat propagation was found to be proportional to time, which is in contrast to the square root of time dependence of the heat diffusion predicted by the ordinary conduction theory.[6] As first pointed out by Anisimov *et al* for a semi-infinite metal surface under the strike of ultrashort laser pulses, the evolution of the electron temperature ($T_{\rm e}$) and the lattice temperatures ($T_{\rm i}$) can be described by the well-known two-temperature model (TTM):[7,8]

$$C_{\rm e}(T_{\rm e})\frac{\partial T_{\rm e}}{\partial t}=\frac{\partial}{\partial x}\kappa(T_{\rm e})\frac{\partial T_{\rm e}}{\partial x}-g(T_{\rm e}-T_{\rm i})+S(x,t), \quad (1a)$$

$$C_{\rm i}\frac{\partial T_{\rm i}}{\partial t}=g(T_{\rm e}-T_{\rm i}), \quad (1b)$$

where x is the direction perpendicular to the surface, $S(x,t)$ is the laser heat source, $C_{\rm e}(T_{\rm e})$ and $C_{\rm i}$ are the heat capacities of the electron and lattice, respectively, g is the heat transfer rate from electrons to the lattice, and $k(T_{\rm e})$ is the electron thermal conductivity, which in fact is contributed by both electron–phonon (e–ph) and electron–electron (e–e) collisions.

In most theoretical treatments, only e–ph collisions are taken into account for the electron diffusion process during and after ultrafast laser pulse heating. For example, Corkum *et al* explained the pulse width dependence of optical damage threshold on polished Cu and Mo surfaces and they obtained an expression of the critical pulse width that distinguishes two different ablation regimes using longer ($\geq$ ns) and shorter ($\leq$ ps)pulse lasers, respectively.[9] With an assumption of a constant electron thermal conductivity based on e–ph collision domination, Nolte *et al* also derived different logarithmic rules between the ablation yield and the laser fluence for subpicosecond-pulse laser ablation of metals.[10] By considering an optional electron heat diffusions, they described approximately

*Project supported by the National Natural Science Foundation of China (Grant No 60378007).
†E-mail: jjyang@nankai.edu.cn

the experimental results. However, the recent pump–probe measurements have revealed that the role of e–e collisions becomes essential for the electron relaxation at electron temperatures around or above 1 eV.[11−13] The e–ph collision dominant electron diffusions are valid only in the low electron temperature regime. Thus, an improved understanding of the impact of e–ph and e–e collisions on the electron diffusion process is crucial for determining some fundamental properties such as thermal electron transport, electron state equations and phase transitions in the scope of laser ablation with ultrafast laser pulses.

In this paper, we extend the conventional two-temperature model from the low temperature regime dominated by e–ph collisions to the high temperature regime through modifying the electron thermal conductivity associated with the e–e collisions. The temporal and spatial evolutions of the electron temperature are investigated in detail for both low and high temperature regimes, and different scaling laws of the electron diffusion are proposed. Pertinent to a practical example of ultrashort laser ablation of a copper target where e–e collisions are considered to play a dominant role in electron diffusions, we derive the dependence of the ablation depth per pulse on laser fluence within the range of $0.1 - 10$ J/cm^2 for different pulse widths. The calculated results show a better consistently with the published experimental data. Although our calculations are based on copper, the main conclusions drawn from this study should be applicable to other metallic materials.

2. Theoretical considerations

According to the two-temperature model described in Ref.[8], the electron temperature evolution at a metal surface excited by ultrafast laser pulses is primarily determined by the two competing processes, namely the electron–ion energy coupling and the electron thermal diffusion. During an electron cooling time $\tau_{\rm R} = C_{\rm e}/g$, which is usually between a few hundred femtoseconds to tens of picoseconds depending on the material, hot electrons tend to transfer their energy to the nearby ion cores, leading to the increase of the lattice temperature, whereas electron diffusions occur simultaneously tending to carry the energy farther away into space. When the laser pulse duration $\tau_{\rm L}$ is much shorter than the characteristic time $\tau_{\rm R}$, only electrons are energized. During the time $t < \tau_{\rm R}$, the electron–lattice coupling can be neglected and the lattice remains unheated. Therefore, the electron thermal diffusion may be regarded as the main energy relaxation process during this stage.

Normally, the thermophysical properties of electrons such as the heat capacity, cooling time and thermal conductivity are all temperature dependent. The electron heat capacity is usually a linear function of the electron temperature given by $C_{\rm e}(T_{\rm e}) = C'_{\rm e}T_{\rm e}$, with $C'_{\rm e}$ being a constant. The electron thermal conductivity can be described generally by $\kappa(T_{\rm e}) = C_{\rm e}v_{\rm F}^2\tau/3$, with $v_{\rm F}$ being the Fermi velocity, which indicates that the thermal conductivity of electrons is linearly proportional to the electron temperature and the electron momentum relaxation time τ (also called transport time). In general, for good conductors, the e–e collision rate may be determined by $v_{\rm e-e} = AT_{\rm e}^2$ whereas the e–ph collision rate is independent of $T_{\rm e}$, but proportional to $T_{\rm i}$, namely, $v_{\rm e-ph} = BT_{\rm i}$. Here A and B are constants, and both contribute to the electron collision frequency ν.[14] A relationship between the electron momentum relaxation time τ and the e–e and e–ph collision rates for electron temperatures below the Fermi temperature is given by[14,15]

$$\frac{1}{\tau} = \nu = v_{\rm e-ph} + v_{\rm e-e} = BT_{\rm i} + AT_{\rm e}^2. \qquad (2)$$

At room temperature we have $v_{\rm e-ph} \approx 10^{14}$ s^{-1} and $v_{\rm e-e} \approx 10^{12}$ s^{-1} so that the electron thermal conduction in this case is dominated by e–ph collisions. On the other hand, at higher electron temperatures $v_{\rm e-e} \approx 10^{15}$ s^{-1} and electron transport properties are primarily governed by e–e collisions. Substituting Eq.(2) into the expression of the electron thermal conductivity, we can obtain the following equation:

$$\kappa = \frac{v_{\rm F}^2 C'_{\rm e}T_{\rm e}}{3}\frac{1}{AT_{\rm e}^2 + BT_{\rm i}} = \kappa_0\frac{BT_{\rm e}}{AT_{\rm e}^2 + BT_{\rm i}}, \qquad (3)$$

where $\kappa_0 = v_{\rm F}^2 C'_{\rm e}/(3B)$ is in fact the electronic heat conductivity at room temperature ($T_{\rm e} = T_{\rm i} = 300$ K).[16] In general, Eqs.(1a) and (1b) can be solved only numerically. To obtain analytic solutions, we will consider a limiting case of $t < \tau_{\rm R}$ wherein in Eq.(1a) only the first term on the right-hand side is important. To model a more realistic situation, a Gaussian laser pulse is assumed with

$$I(t) = [F_0/\sqrt{\pi}\tau_{\rm p}]\exp(-t^2/\tau_{\rm p}^2),$$

with F_0 being the absorbed laser fluence. The electron temperature evolvement in two different regimes is demonstrated as follows.

2.1. Low electron temperature regime

If the laser-induced electron temperature T_e is relatively low so that the condition of $BT_i \gg AT_e^2$ is fulfilled, the electron diffusion process will be dominated by e–ph collisions. In such a case, the electron thermal conductivity κ may be simplified to $\kappa \approx \kappa_0 T_e/T_i$, which has been widely used by many authors in the two-step heating model.[9,10] Now Eq.(1a) becomes an ordinary diffusion equation for T_e^2,

$$C'_e \frac{\partial}{\partial t}(T_e^2) = \frac{\kappa_0}{T_i}\frac{\partial^2}{\partial x^2}(T_e^2) + S(x,t). \tag{4}$$

An analytic solution of Eq.(4) can be readily derived[9]

$$T_e\Big(x,t\Big) = \Big(\frac{4T_i}{\pi\,\kappa_0 C'_e}\Big)^{1/4}\Big(\frac{F_0^2}{t}\Big)^{1/4} \times \exp\Big(-\frac{C'_e T_i}{4\,\kappa_0 t}x^2\Big)^{1/2}. \tag{5}$$

The evolution of surface electron temperature is thus given by

$$T_e(0,t) = \Big(\frac{4T_i}{\pi\,\kappa_0 C'_e}\Big)^{1/4}\Big(\frac{F_0}{\tau_p}\Big)^{1/2}(t)^{1/4}, \quad (t \le \tau_p), \tag{6a}$$

$$T_e(0,t) = \Big(\frac{4T_i}{\pi\,\kappa_0 C'_e}\Big)^{1/4}\Big(F_0\Big)^{1/2}\Big(\frac{1}{t}\Big)^{1/4}, \quad (t > \tau_p). \tag{6b}$$

From Eqs.(6), the time dependence of electron heat diffusion length can be obtained as follows:

$$L_T(t) = \Big(\frac{2\kappa_0}{C'_e\,T_i}t\Big)^{1/2}. \tag{7}$$

This is similar to the common expression in estimating heat diffusion length for the conventional nanosecond or longer-pulsed laser ablation. However, here we have the electron diffusion coefficient, which may be defined as $2\kappa_0/C'_e T_i$ instead of the phonon diffusion coefficient. In this case, The electron diffusion length is linearly proportional to the square root of time, $L_T \sim t^{1/2}$, independent of laser fluence. The electron thermal diffusivity $\chi = \kappa/C_e$ is approximately constant, and the heat front velocity is governed by $\upsilon_T = L_T/t = (2\kappa_0/C'_e T_i\,t)^{1/2}$, which reduces linearly as the square root of time increases. Moreover, the electron cooling time τ_R in this case can be expressed by

$$\tau_R = \frac{C'_e\,T_e}{g} = \Big(\frac{4T_i\,C'^3_e F_0^2}{\kappa_0 \pi\, g^4}\Big)^{1/5}. \tag{8}$$

If the characteristic electron diffusion depth L_R is defined as a length of the electron diffusion at $t = \tau_R$, we can have the following form by combining Eq.(7) with Eq.(8)

$$L_R = 2\Big(\frac{1}{8\pi}\Big)^{1/10}\Big(\frac{\kappa_0^2 F_0}{T_i^2 g^2 C'_e}\Big)^{1/5}. \tag{9}$$

This equation shows that the characteristic electron diffusion depth grows with increasing laser fluence before hot electrons finish their energy transfer to the lattice.

2.2. High electron temperature regime

When the laser-induced electron temperature T_e becomes higher, the condition of $AT_e^2 \gg BT_i$ may be satisfied, and the electron diffusion process enters into the regime dominated by e–e collisions. In this case, the electron thermal conductivity κ can be reduced to $\kappa \approx \kappa_0 B/AT_e$. By substituting κ into Eq.(1a), we can obtain

$$C'_e T_e \frac{\partial T_e}{\partial t} = \frac{\kappa_0}{(B/A)^{-1}}\frac{\partial}{\partial x}(T_e^{-1})\frac{\partial T_e}{\partial x} + S(x,t). \tag{10}$$

The general analytic solution for this type of equation with ultrafast laser energy deposition has been derived by Kanavin *et al*,[17] which can be written as

$$T_e(x,t) = \Big(\frac{8A}{\pi^2 C'_e \kappa_0 B}\Big)^{1/2}\Big(\frac{F_0^2}{t}\Big)^{1/2} \times \left(\frac{L_T^2(t)}{(x+\upsilon_T\tau_p)^2 + L_T^2(t)}\right)^{1/2}, \tag{11}$$

where $L_T(t)$ is the heat diffusion length of electrons, and it has the following form

$$L_T(t) = \begin{cases} \dfrac{\pi\,B\kappa_0}{2A}\dfrac{\tau_p}{F_0}, & (t \le \tau_p) \\ \dfrac{\pi\,B\kappa_0}{2A}\dfrac{t}{F_0}, & (t > \tau_p). \end{cases} \tag{12}$$

Here we can see that the electron diffusion length during the laser–matter interaction time is proportional to the laser pulse width but is not time dependent. The longer the pulse duration is, the greater the electron diffusion becomes. While after the laser–matter interaction the electron diffusion length increases linearly with time, $L_T - t$. In both situations, the electron diffusion length is inversely proportional to the absorbed laser fluence at any time, $L_T - 1/F$, which means that the laser irradiation with higher laser fluences makes the electron diffusion smaller. Additionally, the electron thermal diffusivity becomes temperature dependent, $\chi = \kappa_0 B/C'_e A T_e^2$, and the

heat propagation velocity also varies in a complicated manner: it decreases linearly with time over the time span of the pulse, $\upsilon_{\rm T} - 1/t$, but seems to be independent of time after the pulse. The dependence of the electron heat propagation velocity on the laser fluence may be expressed as $\upsilon_{\rm T} - 1/F$, which suggests that high laser fluences lead to a decrease of the electron diffusion speed, resulting in an increased spatial concentration of the absorbed laser energy. Obviously, such an electron diffusion behaviour based on e–e collisions is greatly different from that based on e–ph collisions. In the e–e collision dominated regime, the scaling laws for the surface electron temperature can be derived from Eq.(11) ,

$$T_{\rm e}(0,t) = \begin{cases} \Big(\dfrac{8A}{\pi^2 C'_{\rm e}\kappa_0 B}\Big)^{1/2}\Big(\dfrac{F_0}{\tau_{\rm p}}\Big)\Big(\dfrac{t^3}{t^2+(t+\tau_{\rm p})^2}\Big)^{1/2}, & (t \le \tau_{\rm p}), \\ \Big(\dfrac{8A}{\pi^2 C'_{\rm e}\,\kappa_0 B}\Big)^{1/2} F_0\Big(\dfrac{t}{t^2+(t+\tau_{\rm p})^2}\Big)^{1/2}, & (t > \tau_{\rm p}). \end{cases} \tag{13}$$

Similar to Eq.(8), the analogous expression for the electron cooling time $\tau_{\rm R}$ in this case can be written as

$$\tau_{\rm R} = \Big(\frac{4AC'_{\rm e}F_0^2}{\pi^2 B\kappa_0\, g^2}\Big)^{1/3}, \tag{14}$$

and the characteristic electron diffusion depth at $t = \tau_{\rm R}$ can be obtained from the following expression:

$$L_{\rm R} = \Big(\frac{\pi B^2\kappa_0^2 C'_{\rm e}}{2A^2 g^2 F_0}\Big)^{1/3}, \tag{15}$$

Equation (15) indicates us that the characteristic electron diffusion depth in the e–e collision regime decreases with increasing laser fluence, in contrast to that in the e–ph collision regime.

3. Numerical analyses and discussions

Some physical parameters used in our simulation of the electron temperature evolution and the heat transport in copper films irradiated by femtosecond laser pulses are summarized in Table 1.

Table 1. Physical parameters used in our calculations for copper material[16,18−20]

Parameter	Units	Value
$T_{\rm i}$ lattice room temperature	K	300
$C'_{\rm e}$ coefficient of the electron heat capacity	$\rm J/(m^3\cdot K^2)$	96.6
$C_{\rm i}$ lattice heat capacity	$\rm J/(m^3\cdot K)$	3.5×10^6
g electron–lattice coupling constant	$\rm W/(m^3\cdot K)$	1×10^{17}
κ_0 electronic heat conductivity at room temperature	$\rm W/(K\cdot m)$	400
A coefficient of electron–electron collision frequency	$\rm K^{-2}\cdot S^{-1}$	1.75×10^7
B coefficient of electron–phonon collision frequency	$\rm K^{-1}\cdot S^{-1}$	1.98×10^{11}
$\upsilon_{\rm F}$ Fermi velocity	m/s	1.57×10^6

In order to find the corresponding electron heat diffusion dynamics in the two regimes dominated by e–ph and e–e collisions, we designate $T_{\rm e}^*$ as a characteristic electron temperature at which the e–e collision rate becomes significantly greater than the e–ph collision rate, namely

$$\frac{AT_{\rm e}^{*\,2}}{BT_{\rm i}} \ge 10\,. \tag{16}$$

This expression indicates that the electron diffusion will be governed by e–e collisions when the electron temperature $T_{\rm e} \ge T_{\rm e}^*$. Otherwise, it will be determined by e–ph collisions. With the tabulated parameters for copper material in Table 1, the characteristic electron temperature is estimated to be in the order of $T_{\rm e}^* \approx 6\times10^3$ K. By using Eq.(6a) under a given laser fluence, we can obtain a characteristic pulse width $\tau_{\rm p}^*$ corresponding to the attainable electron temperature $T_{\rm e}^*$. For example, at $F^* \approx 16.3$ mJ/cm^2, we can obtain $\tau_{\rm p}^* \sim 100$ fs. Variation of the characteristic pulse width versus laser fluences for reaching the electron temperature $T_{\rm e}^*$ is plotted as the solid curve in Fig.1, where the region above the curve represents the elec-

tron diffusion with dominant contribution from e–ph collisions, while the region below the curve is associated with the electron diffusion governed by e–e collisions. This result also indicates a fact that for a given absorbed laser fluence, there always exists a characteristic pulse width $\tau_{\rm p}^*$ to gain $T_{\rm e} = T_{\rm e}^*$. If $\tau_{\rm p} \leq \tau_{\rm p}^*$, the electron temperature has $T_{\rm e} \geq T_{\rm e}^*$, and the electron diffusion will be dominated by e–e collisions.

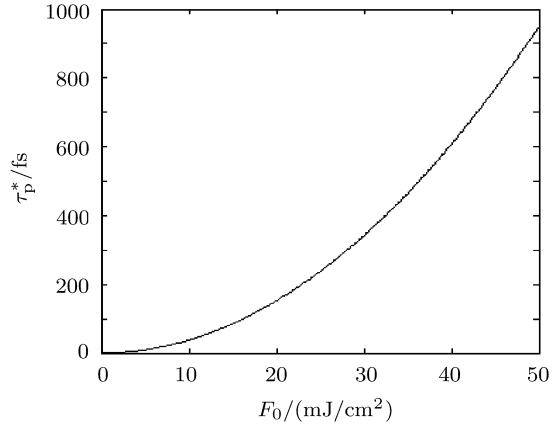


Fig.1. The variation of pulse width and the laser fluence for achieving the characteristic electron temperature $T_{\rm e}^*$

The pulse-width dependence of the maximum electron temperature at copper surface for a given laser fluence of $F_0 = 16.3$ mJ/cm^2 is illustrated in Fig.2(a). It can be seen that the maximum surface electron temperature in e–e collision regime is strongly dependent on the pulse duration. The shorter the pulse width is, the higher the electron temperature becomes. Instead, a relatively slowly decreasing tendency of the calculated curve in e–ph collision regime for $\tau_{\rm p} > \tau_{\rm p}^*$ indicates that the electron temperature is much less related to the pulse duration. Figure 2(b) shows the dependence of the maximum electron temperature on laser fluence at the copper surface impinged by a 100 fs laser pulse. Dramatically different variation patterns of $T_{\rm e\,max}$ with increasing laser fluence can be observed in the two different laser fluence ranges separated by F_0*. This means that the available highest electron temperature is much more sensitive to the laser fluence in the e–e collision regime than in the e–ph collision regime.

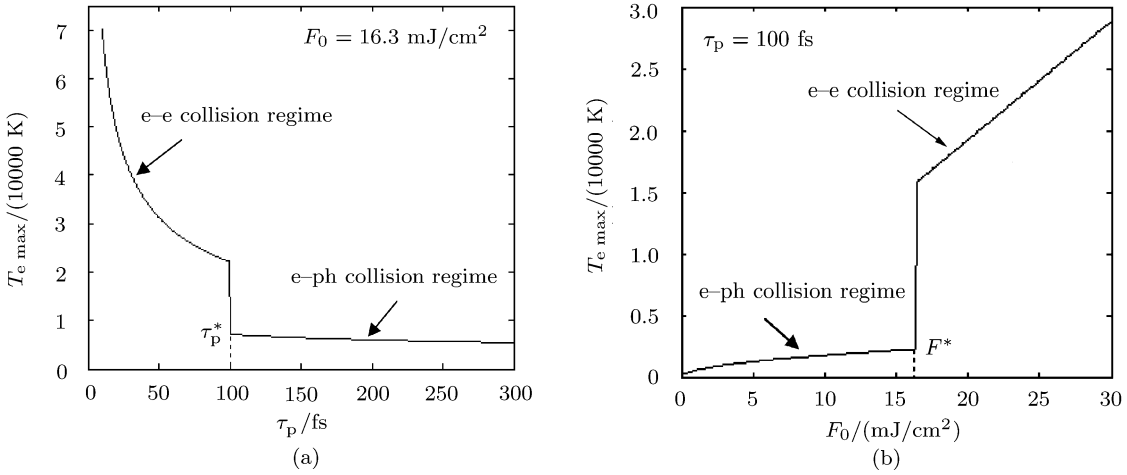


Fig.2. Variation of the maximum electron temperature at copper surface in e–e and e–ph collision regimes as a function of pulse duration for a given laser fluence of 16.3 mJ/cm^2 (a), and of laser fluence for a given pulse duration of 100 fs (b).

In order to obtain a clear physical picture of the electron diffusion dynamics in the two distinct regimes, we calculate the dependence of the electron diffusion length on the elapsing time associated with a 100 fs laser pulse under different laser fluences. The calculated results are shown in Fig.3. When the absorbed laser fluence F_0 satisfies $F_0 \leq F^*$, a relatively large electron diffusion length occurs in e–ph collision dominant regime, and it grows rapidly as the time elapses. Consequently, this drastic change of the electron diffusion length with time will inevitably result in some negative effects, such as enlargement of the heat affected zone, the decrease of the temperature at the surface and reduction of the ablation efficiency. However, for $F_0 > F^*$, e.g. $F_0 = 18$, or 25 mJ/cm^2, the electron diffusion length is relatively small. Especially during the laser–matter interaction period, the electron diffusion length remains almost unchanged with time but reduces with laser fluence. As a result of negligible hot electron diffusions, the absorbed laser energy will be deposited or 'frozen' within a very thin surface layer at this pulse width. Obviously, this will

lead to a much higher surface temperature, and thus improve the heating efficiency greatly. This kind of the electron diffusion behaviour is more favourable for high-precision femtosecond laser ablation. However, after the laser pulse the electron diffusion length increases linearly with time, and the heat propagation speed decreases with increasing laser fluence. These diffusion features are in sharp contrast to that in the case of $F_0 \leq F^*$.

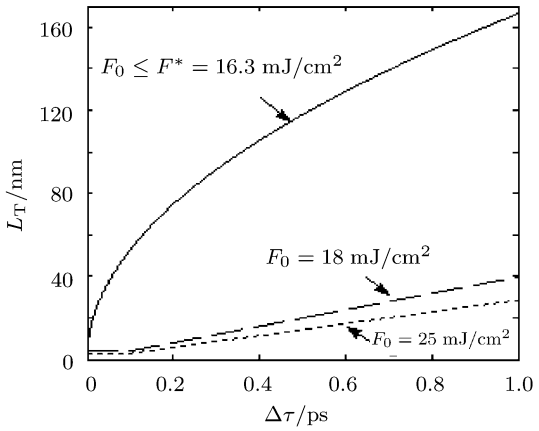


Fig.3. Heat penetration depth as a function of elapsed time during and after100 fs laser pulse heating in e–ph collision regime (solid), and in e–e collision regime (dashed and dotted).

Figure 4 shows the dependence of the characteristic electron diffusion depth L_R on laser fluence in both regimes. In this figure, the change of the electron diffusion depth is found to have two opposite tendencies with the increase of laser fluence. The increasing characteristic electron diffusion depth with higher laser fluences in e–ph collision regime suggests that the absorbed laser energy is dissipated seriously in space, while the decreasing characteristic electron diffusion depth with higher laser fluences in e–e collision regime indicates that the heating efficiency of the lattice is improved.

Figure 5 shows the electron temperature profiles along the direction normal to the sample surface at the time delay of 1 ps for two selected laser fluences, one is higher and the other is lower than the characteristic value F^*, but both correspond to the same pulse width of 100 fs. Clearly, the spatial electron temperature distributions are very different in these two cases. When the laser fluence satisfies $F_0 > F^*$, e.g. $F_0 = 20$ mJ/cm^2, the electron temperature has a steeper spatial distribution. In other words, it deceases fast with the diffusion depth. The higher electron temperature within a narrower spatial range means that most of the absorbed laser energy is confined within a very small volume because of weaker electron diffusion. In contrast, for the case of low laser fluence, $F_0 = 12$ mJ/cm^2, the spatial electron temperature distribution becomes relatively flatter, indicating that the absorbed laser energy spreads widely in a larger volume and the electron diffusion becomes stronger.

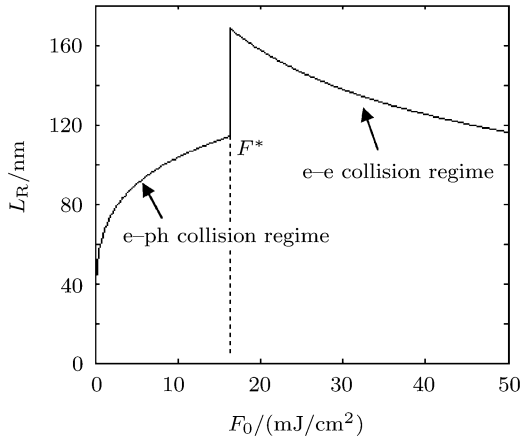


Fig.4. The critical electron deposition depth as a function of laser fluence for a 100 fs pulse in the e–e and e–ph collision regimes.

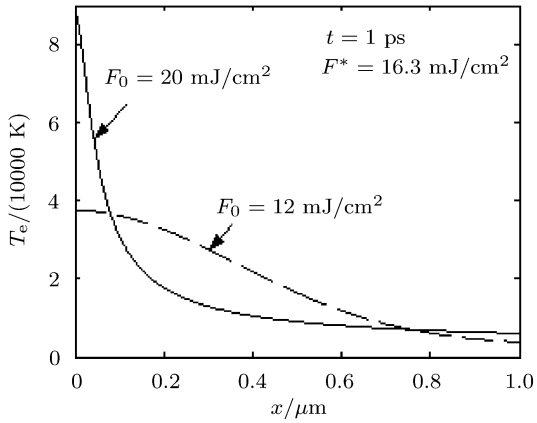


Fig.5. The spatial distributions of electron temperature for a given laser pulse width of 100 fs at 1 ps time delay in e–e and e–ph collision regimes.

Figure 6 shows the time required to reach the maximum electron temperature as a function of the laser fluence at the location $d = 100$ nm in both e–e and e–ph collision regimes. The constant time delay in the e–ph collision regime ($F_0 \leq F^*$) suggests that the electron heat propagation velocity remains constant for different laser fluences. However, when the e–e collisions become dominant ($F_0 > F^*$), the time delay grows proportional to the laser fluence, which

indicates that the electron heat propagation velocity reduces with increasing laser fluence.

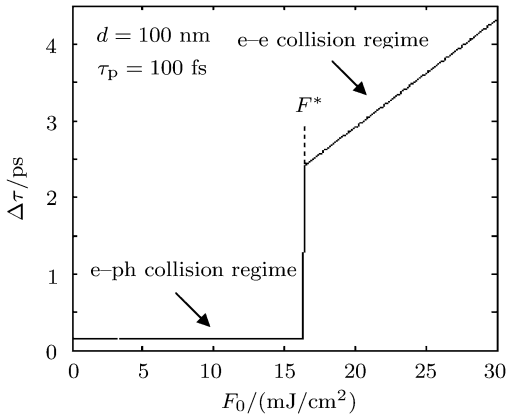


Fig.6. The time required to reach the maximum electron temperature as a function of the laser fluence at the location $d = 100$ nm in both e–e and e–ph collision regimes.

4. Calculated results versus experimental data

So far, we have presented some detailed analyses on the 'unusual' electron diffusion process contributed by e–e collisions associated with high laser fluence irradiation. To confirm that the analyses presented above can indeed help us to gain better understanding of the dynamics of ultrafast laser ablation of metallic targets, now let us simulate the ablation behaviours revealed in the experiment.[10] The calculated results of the ablation rate as a function of the laser fluence ranging from 100 mJ/cm^2 to 10 J/cm^2 for different pulse widths are reproduced in Fig.7 together with the corresponding experimental data obtained from Ref.[10]. To account for the material removal from the target surface, electron diffusions dominated by e–e collisions are considered to be followed by energy coupling between the electron and lattice. Subsequently the lattice temperature at the time of relaxation can be achieved with the help of Eq.(2). When its available value is close to the thermodynamic equilibrium critical point T_c, ablation is assumed to occur under phase explosion.

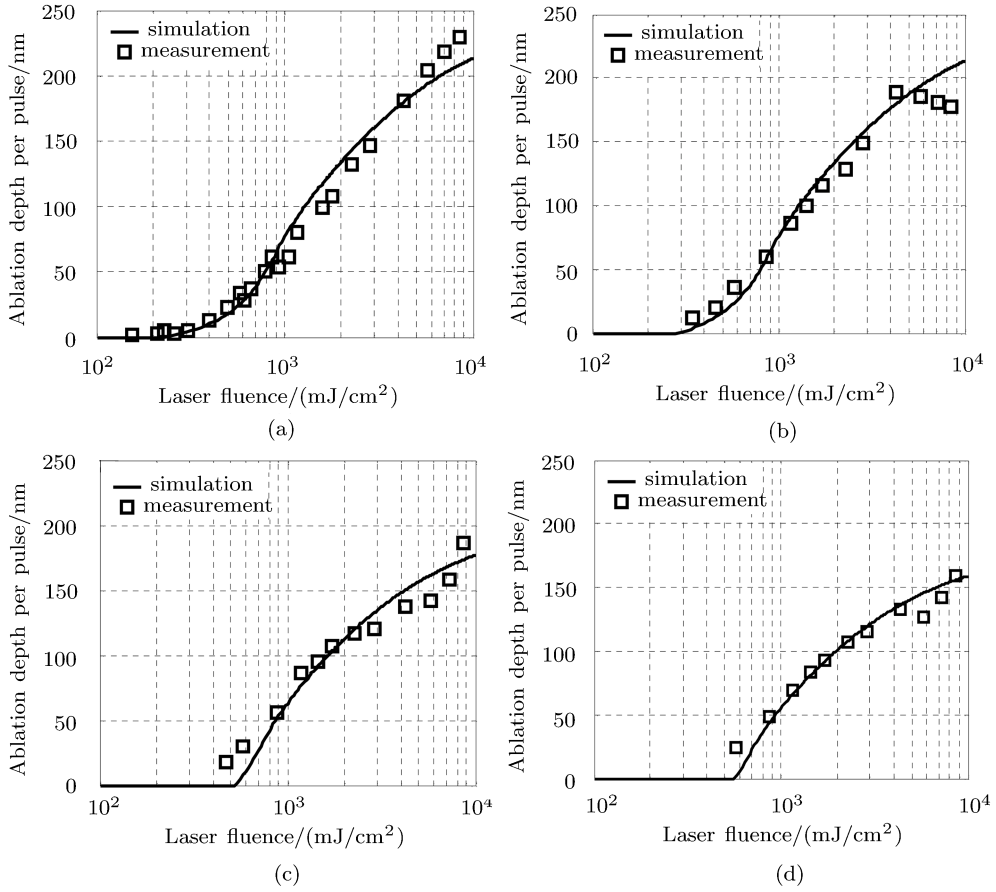


Fig.7. Simulated (solid curve) and experimental (squares) data by Nolte *et al* of the ablation yield as a function of laser fluence for copper with 500 fs (a), 1 ps (b), 7.6 ps (c) and 9.6 ps (d) incident laser pulses.

Therefore, the ablation depth can be calculated from the spatial temperature distribution in the lattice above the value of T_c at the time of τ_R. The graphs shown in Figs.7(a), 7(b), 7(c) and 7(d) are for 500 fs, 1 ps, 7.6 ps and 9.6 ps laser pulses respectively. As it can be seen clearly, in all the four cases which represent a large range of pulse duration, the calculated results fit very well with the experimental data. In particular, the calculated ablation threshold fluences in all these graphs are very close to the experimental ones. With the augment of pulse width, the threshold fluence increases. For a given laser fluence, the ablation rate decreases for broader pulses. It is worth to note that all the calculated curves shown in Fig.7 are rather smooth without introducing and complying with separate ablation rules. This is in great contrast to the simulation works given earlier,[10,21] in which two separated fitting curves based on different electron diffusion mechanisms have been employed to match the measured results. Also, by considering the dominant contribution from e–e collisions to electron thermal diffusions, we have successfully simulated the dependence of the critical pulse width on laser fluence, predicting the existence of two distinct ablation regimes related to thermal and non thermal ablations of metallic materials with ultrashort laser pulses. The simulation results are in good consistency with the experimental data.[22]

5. Conclusion

In summary, this paper has presented some detailed theoretical analyses of the electron diffusion dynamics for ultrashort laser pulse heating of metallic targets. The electron diffusion process has been divided into e–ph collision and e–e collision regimes depending on the electron temperature through modifying the conventional two-temperature equations. The main features of the electron diffusion laws in both regimes have been compared and discussed by using numerical calculations. It has been shown that in e–ph collision regime the electron diffusion behaviours including the electron relaxation time, thermal diffusivity, the heat propagation speed and the heat penetration length, are all independent of the laser-fluence for a given pulse width, whereas in e–e collision regime these parameters are almost inversely dependent on the laser fluence, which is likely more favourable for making high-precision ablations. Finally, by assuming the electron diffusion process dominated by e–e collisions under the high laser fluence irradiation, we have accomplished simulations of the laser fluence dependent ablation rate at different laser pulse widths on copper targets. Excellent agreements between our calculated results and the published experimental data indicate that the theoretical model we proposed is a useful tool for gaining a better understanding of ultrafast electron diffusion kinetics in ultrashort-pulse laser ablation of metals.

References

[1] Fujimoto J G, Liu J M, Ippen E P and Bloembergen N 1984 *Phys. Rev. Lett.* **53** 1837

[2] Zhao Q Z, Qiu J R, Zhao C H, Jiang X W and Zhu C S 2005 *Chin. Phys.* **14** 1181

[3] Li C B, Jia T Q, Sun H Y, Li X X, Xu S Z, Feng D H, Wang X F, Ge X C and Xu Z Z 2006 *Acta Phys. Sin.* **55** 217 (in Chinese)

[4] Elsayed-Ali H E and Juhasz T 1993 *Phys. Rev.* B **47** 13599

[5] Brorson S D, Fujimoto J G and Ippen E P 1987 *Phys. Rev. Lett.* **59** 1962

[6] Chichkov B N, Momma C, Nolte S, Alvensleben F and Tünnermann A 1996 *Appl. Phys.* A **63** 109

[7] Anisimov S I, Bonch-Bruevich A M, Elyashevich M A, Imas Y A, Pavlenko N A and Romanov G S 1967 *Sov. Phys. Tech. Phys.* **11** 945

[8] Anisimov S I, Kapeliovich B L and Perelman T L 1974 *Sov. Phys. JETP* **39** 375

[9] Corkum P B, Brunel F and Sherman N K 1988 *Phys. Rev. Lett.* **61** 2886

[10] Nolte S, Momma C, Jacobs H and Tünnermann A 1997 *J. Opt. Soc. Am.* B **14** 2716

[11] Fann W S, Storz R, Tom H K and Bokor J 1992 *Phys. Rev.* B **46** 13592

[12] Sun C K, Vallee F, Acioli L, Ippen E P and Fujimoto J G 1993 *Phys. Rev.* B **48** 12365

[13] Sun C K, Vallee F, Acioli L, Ippen E P and Fujimoto J G 1994 *Phys. Rev.* B **50** 15337

[14] Anisimov S I and Rethfeld B 1997 *Proc. SPIE* **3093** 192

[15] Wang X Y, Riffe D M, Lee Y S and Downer M C 1994 *Phys. Rev.* B **15** 8016

[16] Schafer C, Urbassek H M and Zhigilei L V 2002 *Phys. Rev.* B **66** 115404

[17] Kanavin A P, Smetanin I V, Isakov V A, Afanasiev Y V, Chichkov B N, Wellegehausen B, Nolte S, Momma C and Tünnermann A 1998 *Phys. Rev.* B **57** 14698

[18] Elsayed-Ali H E, Norris T B, Pessot M A and Mourou G A 1987 *Phys. Rev. Lett.* **58** 1212

[19] Wang Z G, Dufour C, Paumier E and Toulemonde M 1994 *J. Phys. Condens. Matte.* **6** 6733

[20] Kaveh M and Wiser N 1984 *Adv. Phys.* **33** 257

[21] Furusawa K, Takahashi K, Kumagai H, Midorikawa K and Obara M 1999 *Appl. Phys.* A **69** S359

[22] Yang J J, Zhao Y B and Zhu X N 2006 *Appl. Phys. Lett.* **88** 094101